SILICON PURIFICATION USING A Cu-Si ALLOY SOURCE

R. C. Powell, P. Tejedor, and J. M. Olson
Solar Energy Research Institute
Golden, CO 80401

ABSTRACT

Production of 99.9999% pure silicon from 98% pure metallurgical-grade silicon by a vapor-transport filtration process (VTF) is described. The VTF process is a cold-wall version of an HCl chemical vapor transport technique using a $Si:Cu_3Si$ alloy as the silicon source. The concentration, origin, and behavior of the various impurities involved in the process were determined by chemically analyzing alloys of different purity, the slag formed during the alloying process, and the purified silicon. Atomic absorption, emission spectrometry, inductively coupled plasma, spark source mass spectrometry, and secondary ion mass spectrometry were used for these analyses. The influence of the Cl/H ratio and the deposition temperature on the transport rate was also investigated.

INTRODUCTION

A large fraction of the cost of a silicon solar cell can be attributed to the cost of the high-purity silicon feedstock or polysilicon. The silicon feedstock problem is likely to persist in the near future since the price of polysilicon appears to be driven by the supply and demand cycles of the electronics industry, the needs of which are not totally compatible with that of the photovoltaics industry.

In 1981, Olson and Carleton (1) invented a process for purifying silicon that combined the silicon filtration properties of Cu_3Si with a molten salt electrorefining process. This process produced a 99.9995 a/o pure silicon capable of yielding solar cells with an efficiency of 12.2% relative to a baseline of 11.9% (2). Later, Olson and Powell developed a vapor transport technique (3-4) that not only lacks the practical problems associated with the molten salt electrolyte but is more efficient and easier to implement on a production scale. The vapor-transport filtration (VTF) process for purifying metallurgical-grade silicon is based on the chemistry of the Si:Cl:H system and combines the filtration properties of Cu_3Si with the chemical selectivity of a closed-cycle HCl vapor transport process to produce 99.9999% pure silicon. Vapor transport processes are covered in the monograph by Schäfer (5) and hot filament processes for purifying metals were first described by van Arkel and de Boer in 1925 (6). In equilibrium, the temperature and Cl/H ratio determine the silicon solubility in the gas phase for the Si:Cl:H system (7-9). For a given Cl/H ratio, thermal conditions can be established such that silicon will be transported in a closed system in the direction of increasing temperature. Conversely, HCl will transport copper (and certain other impurities) in the opposite direction, precluding the accumulation of copper at the filament (5).

The overall purification is a result of at least four mechanisms: 1) diffusional trapping of impurities in the Cu-Si alloy by slow, solid state diffusion; 2) segregation by the differential action of the HCl chemical vapor transport reactions for the various metal impurities; 3) gettering of impurities by a Cu_2O:SiO_2 slag during the Cu-Si alloying stage; and 4) condensation of metal impurity chlorides on the water-cooled baseplate of the reactor during the vapor-transport stage of the process.

In the following we first briefly describe the apparatus and its operation. The remainder of the paper is devoted to a discussion of the characteristics of the refined silicon including its purity, electronic properties, deposition rate, and morphology. Furthermore, we will attempt to quantify the relative importance of the various mechanisms responsible for the purification efficiency.

EXPERIMENTAL

A schematic of the experimental reactor is shown in Figure 1. The reactor consists of a hot silicon filament surrounded by a battery of Si:Cu_3Si composite alloys. The composite alloys are cast from a hypereutectic solution of metallurgical-grade silicon (mg-Si) and copper to form a two-phase system consisting of a primary silicon phase embedded in a Cu_3Si matrix. The alloys are approximately 5x5x1 cm^3.

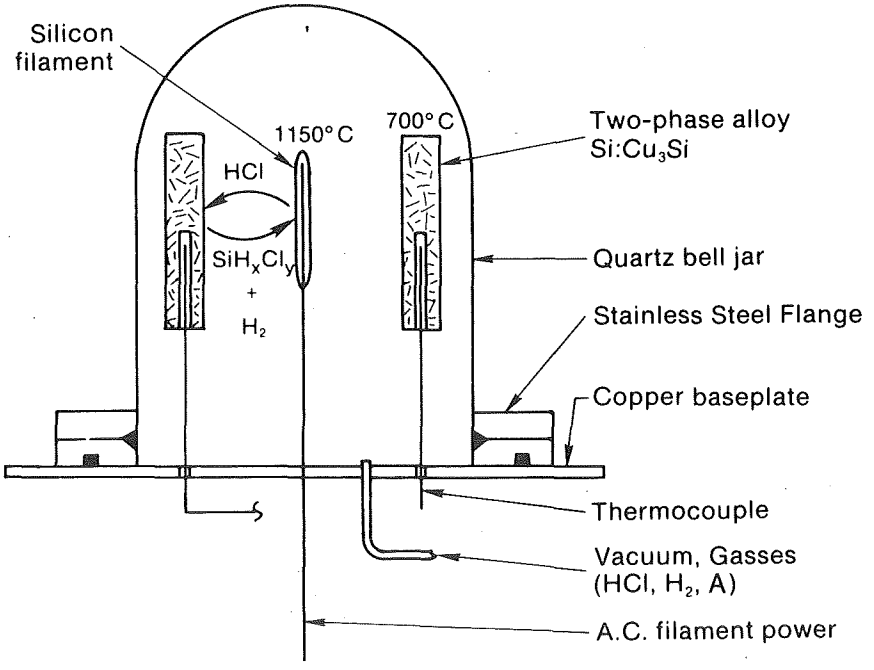

Figure 1. Schematic diagram of the experimental VTF reactor.

Inconel-sheathed thermocouples within embedded graphite wells support the alloys. Graphite fixtures, connected to copper power feedthroughs, support and conduct current to the filament. The filament, made of high-purity Poco® DFP-1 graphite sheet, is clamped between two graphite pieces with graphite screws. A 1.5-liter quartz bell jar encloses the primary components and seals to a copper baseplate by means of a stainless steel flange and Viton O-rings. Both the stainless steel flange and the copper power feedthroughs are water-cooled. Before every run, the reactor is evacuated by means of a turbomolecular pump and outgassed until the pressure is ~30 mtorr. After evacuation, the free space of the reactor is backfilled to atmospheric pressure with a mixture of HCl and H_2. These initial proportions determine the Cl/H ratio. An optical pyrometer is used to measure the filament temperature.

Radiation from the resistively heated filament passively heats the alloys. With the silicon filament at 1100°C and the composite alloy at 700°C, silicon is transported from the alloy to the filament by the following nominal transport reaction:

$$Si + xHCl \underset{1100^{\circ}C}{\overset{700^{\circ}C}{\rightleftarrows}} SiH_{4-x}Cl_x + (x-2)H_2 \ ,$$

where x = 2, 3, and/or 4. The HCl reacts with the Si-Cu alloy to form a mixture of chlorosilanes and hydrogen. These reactants are then transported to the hot silicon filament by a combination of diffusion and convection where they back-react, depositing silicon on the filament and releasing HCl to continue the process. The general process is traditionally called chemical vapor transport (CVT) and is a well-known technique (5).

The deposition of silicon causes the electrical conductance of the filament to change. Since it is very easy to monitor these changes continuously, we have a convenient way to indirectly monitor the filament growth (4,10). If silicon is deposited uniformly on a filament of length L, width W, and thickness X, then the conductance is given by

$$C = \sigma WX/L \ ,$$

where σ is the electrical conductivity of the deposited silicon. This conductivity depends on the doping, the temperature, and the grain structure of the deposited silicon. However, if these factors remain relatively constant, the increase in conductance with time is directly related to the increase in filament thickness and hence filament mass m. Thus,

$$\frac{dC}{dt} = \frac{\sigma}{\rho L^2} \frac{dm}{dt} \ ,$$

where ρ is the mass density of silicon.

As silicon is removed from the surface of the alloy, it must be replenished by the outdiffusion of silicon from the bulk of the two-phase alloy. From the Phase Rule we can show that the outdiffusion silicon must result in a decrease in the concentration of primary silicon particles and the formation of a single-phase (Cu_3Si) depletion layer that grows with time. The run is terminated after the composite alloy has been depleted of its primary silicon.

For convenience, we use a graphite starter filament, which is much easier to ohmically heat than silicon. Therefore, for chemical and electrical analysis, the silicon must be stripped from the graphite filament. Chemical analysis of the refined silicon is made by spark source mass spectrometry on bulk samples cut from lapped sections. The alloys during various stages of the process and the slag formed during the alloying step are analyzed by inductively coupled plasma atomic absorption (ICP) and standard emission spectroscopy. Resistivity measurements are made on lapped, polycrystalline samples and also on single-crystal samples grown by the Czochralski technique from the refined polycrystalline material.

RESULTS AND DISCUSSION

Purity

The alloying process plays an important role in the overall purification. Since the silicon and the copper are alloyed in an open-air furnace with a graphite crucible, a slag of SiO_2 and Cu_2O is formed on the surface of the molten alloy. This slag getters many impurities associated with the metallurgical-grade silicon, resulting in an alloy substantially purer than the starting materials. Table 1 compares the purity of a series of alloys made under different alloying conditions of time t and temperature T. In all cases, the alloys were soaked for 90 and 150 min at temperatures between 1060° and 1300°C for a Cu-Si alloy with an initial metallurgical-grade silicon concentration of 20 w/o. The data indicate that the purity of the alloy generally increases with soaking temperature and decreases with soaking time. The eutectic temperature of the Cu_2O:SiO_2 slag is 1060°C, which explains the rather poor results observed at the 1060°C soaking temperature. At higher temperatures the slag is in the liquid state and at still higher temperatures it becomes less viscous, conditions necessary for efficient gettering. Also, the silicon content of the alloy, compared with the initial proportion, is an inverse function of soaking temperature.

Table 1. Effects of casting conditions on alloy purity

T_{soak} (C)	t_{soak} (min)	Cu (%w)	Si (%w)	Al (ppm)	Cr (ppm)	Fe (ppm)	Mn (ppm)	Ti (ppm)	V (ppm)
1060	90	73.37	25.64	3797	<5	559	30	<70	151
1060	150	76.76	21.31	14953	<5	1220	35	<70	469
1200	90	80.00	19.85	686	<5	181	14	<70	5
1200	150	80.43	19.46	775	5	265	19	<70	5
1300	90	81.35	18.59	512	<9	178	39	190	5

To track the impurities throughout the process, we analyzed by spark source mass spectroscopy, emission spectrometry, and inductively coupled plasma 1) the metallurgical-grade silicon used to form the Cu-Si alloy source, 2) the Cu_2O:SiO_2 slag, 3) a Cu-Si alloy with ~25 w/o Si and soaked at a temperature of 1200°C, 4) the Cu-Si alloy after the VTF process, and 5) the VTF-refined silicon. The results are shown in Table 2. The data indicate that a significant fraction of the impurities in the mg-Si are gettered by the Cu_2O:SiO_2 slag during the alloy-forming process. In particular, the slag is efficient at gettering Al and Ca. At this point, any further segregation of the impurities must be associated with the VTF process, including the condensation, diffusional trapping, and vapor transport mechanisms. The purity of the alloy is essentially unchanged by the action of the VTF process.

Table 2. Typical impurity concentrations (ppm) in mg-Si in the slag, the Cu/mg-Si alloy before and after the VTF process, and the refined Si.*

Impurity	mg-Si	Slag	Alloy before VTF (ppm)	Alloy after VTF	Refined Si
Al	1400	1800	50	<10	<0.1
B	<10	<10	<10	<10	0.5
Ba	20	30	<10	<10	<0.02
Ca	235	365	<10	<10	0.07
Cr	185	95	55	55	<0.05
Cu	---	---	$\sim 8.7 \times 10^5$	---	0.12-0.15
Fe	3150	1200	720	690	<0.08
Mg	15	25	<10	<10	0.12
Mn	755	325	155	60	0.05
Mo	<10	<10	<10	<10	0.03
Ni	30	30	<10	<10	0.14-0.57
P	<10	105	45	<10	0.15-1.8
Ti	260	105	45	40	<0.06
V	195	105	40	30	<0.05
Zr	195	70	10	10	<0.04

*mg-Si = metallurgical-grade silicon

Some segregation of impurities is likely to occur in most vapor transport systems of this type. This segregation is determined by the enthalpy change of the relevant transport reaction. Exothermic reactions, like those involving HCl and Si, transport the solid to the hot filament. Endothermic reactions and physical vapor transport tend to accumulate the deposit at the coolest point in the system (see Figure 2). For example, the HCl transport reaction for copper is probably the following endothermic reaction (5):

$$Cu + HCl \underset{700^{\circ}C}{\overset{1100^{\circ}C}{\rightleftarrows}} CuCl + \frac{1}{2} H_2 .$$

The net effect is to transport copper from the "hot" filament to the "cold" alloy source, essentially precluding the accumulation of copper at the filament. But for impurities like B and Al, the segregation (due to the CVT process) should be negligible (4). If these impurities exist at the surface of the alloy, the HCl should transport them to the hot silicon filament.

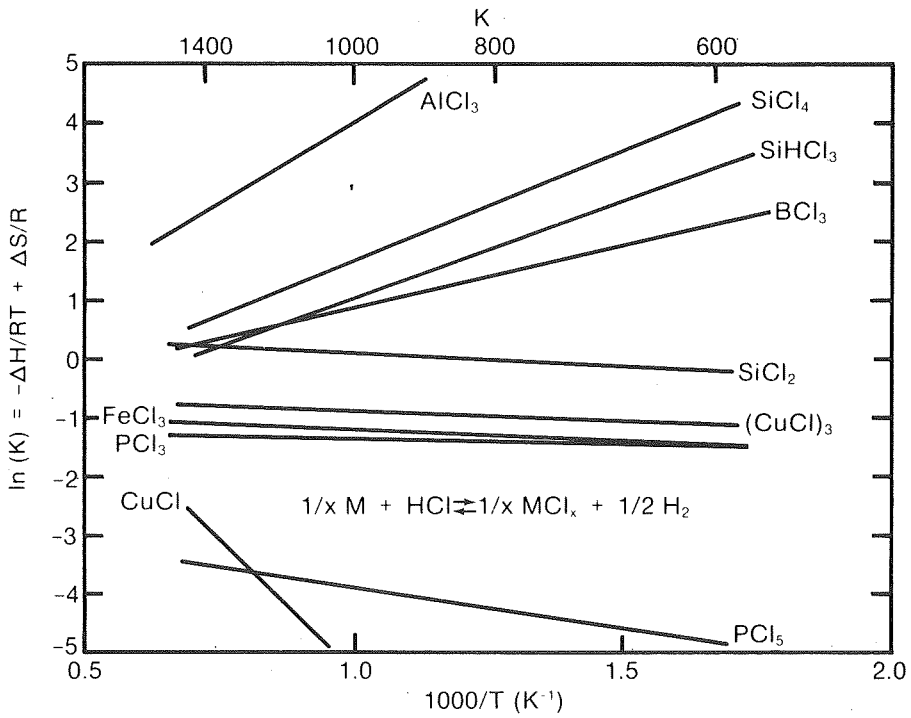

Figure 2. Calculated equilibrium constants for various HCl transport reactions possible as a function of inverse temperature. Exothermic reactions have a positive slope and are expected to transport up the temperature gradient.

The use of a composite Si:Cu_3Si source, however, greatly enhances the segregation of these impurities by limiting the rate at which they can be extracted from the bulk of the source. As a result of the rapid cooling during casting, the impurities originating from either the metallurgical silicon, the copper source, or the alloying crucible are presumably distributed more or less uniformly throughout the alloy (although there may be some enrichment of impurities in the interior). The effective diffusion of silicon in Cu_3Si at 700°C is rapid ($D_{Si} > 10^{-5}$ cm^2/s), while the diffusion of other metal impurities like B, P, Al, and Ti is much slower (2,4,12). Hence, the transport gas HCl, capable of acting only on the surface of the alloy, can extract or transport only silicon at any reasonable rate, leaving behind impurities that otherwise might have been transported to the hot filament. The net effect is that all impurities, independent of their thermochemical properties, are efficiently segregated. The copper concentration in the refined silicon is never larger than 0.1 ppma, illustrating the purification efficiency of the HCl vapor transport process for elements that react endothermically with HCl. Boron is typically less than 0.2 ppma. Boron, aluminum, titanium and phosphorus should be diffusionally trapped within the bulk of the η-Cu_3Si matrix. These, plus other elements such as Fe, Ti, and Mn, are also segregated during the casting step by slagging processes. Compared with the results for the other elements, the residual phosphorus concentration is anomalously high. This residual P concentration could be intrinsic to the process or could be a function of the purity of the reactor/process environment. Finally, the carbon concentration varies from <10 ppma to >100 ppma. This again seems to be a function of reactor purity, since C should not be transported by HCl.

The serendipitous purification mechanism is the condensation of impurity chlorides on the cooled baseplate. Although it is not possible to quantitatively determine the fraction of impurities removed by this mechanism, Al, K, and Mn have been chemically identified. Furthermore, it is not clear whether or not much of this condensate accumulates during cooling of the reactor. In addition, a powdered residue originating on the surface of the alloys accumulates on the baseplate. This residue contains Fe, Al, Ca, Mg, Ti, V, Ni, Mn, and B (4).

To determine the background or baseline for the overall process, a number of different silicon sources were substituted for the mg-Si:Cu alloy source. Alloys made from electronic-grade Si (eg-Si) were considerably purer than alloys made from mg-Si; almost every impurity was below the 10-ppm level. However, the purity of the Si derived from these alloys was essentially the same as that derived from those alloys made with mg-Si. Moreover, deposits made using a pure eg-Si or a mg-Si source were also of similar purity.

Semiconductor Characteristics

The refined silicon material is typically n-type with a resistivity of 0.1-1 ohm-cm. After recrystallization, this material is still n-type with a resistivity of 0.08 ohm-cm. This correlates well with the relative concentration of P and B usually measured by chemical analysis in this material. The Hall mobility is 520 cm^2/Vs with a carrier concentration of $1.5 \times 10^{17} cm^{-3}$.

To determine the photovoltaic quality of the VTF-refined silicon, a single crystal with (111) orientation was grown from 75 g of the VTF material using the Czochralski crystal-growth technique. This 75 g was the product of four separate purification runs. Wafers from the middle of the boule along with 0.2 ohm-cm

wafers from Monsanto and wafers from a grown control boule were simultaneously processed into solar cells. The junctions were formed from a boron spin-on diffusion source with a 30-min drive-in at 906°C. The front and back contacts were of the TiPdAg type with no antireflection coating. The average, total area (0.1 cm^2) efficiency for four cells was 9.6%, with a high of 9.8%. The 9.8% cell had an open-circuit voltage (V_{oc}) of 622 mV, a short-circuit current density (J_{sc}) of 19.6 mA/cm^2, and a fill factor (FF) of 0.81. The control cells had an average efficiency of 9.6%; no cell had a V_{oc} greater than 604 mV. These results are a good indication that this VTF-refined silicon is of solar-grade quality.

Growth Morphology

The morphological stability of the silicon filament is an important process parameter. If the growth morphology of the silicon filament becomes dendritic, the purification efficiency and yield of the process can decrease. This growth morphology is affected by several parameters including temperature, pressure, reactor purity, and growth rate. At filament temperatures much less than 900°C, the growth morphology becomes dendritic. (At temperatures much greater than 1300°C, the growth rate approaches zero.) Good product morphology is favored by initial gas pressures ($P_H + P_{HCl}$) greater than 400-500 torr. Furthermore, oxygen and/or water vapor appear to adversely affect the product morphology.

Deposits on graphite are polycrystalline with a semicolumnar grain structure and a [110] fiber texture. Near the silicon-graphite interface, the grain size is typically on the order of 1-10 μm, and increases with distance from the graphite-silicon interface.

Purification Rate

The purification rate is an important economic parameter. In principle, it is a function of several variables including temperature, pressure, Cl/H, alloy composition and the surface areas of the filament and alloy sources. Under normal operating conditions, however, the purification rate is limited by the rate of diffusion of silicon from the bulk to the surface of the alloy and is therefore most affected by the alloy temperature and surface area.

To study the transport rate, we carried out a series of runs at deposition temperatures of 1050° to 1300°C and with Cl/H ratios between 0.3 and 1.0 at atmospheric pressure. The transport rate was measured using both a time-average method and the real-time, *in situ* method described previously. The time-average transport rate was obtained by dividing the mass deposited by the total run time. Under optimum growth conditions using the Cu-Si alloy, the conductance increases as $t^{1/2}$. Thus, the deposition rate decreases as $t^{-1/2}$. In Figure 3, the filament conductance is plotted as a function of $t^{1/2}$ for a series of runs carried out at four different Cl/H ratios and a filament temperature of 1160°C. We observe a linear behavior in all cases in which good deposits are made at times that extend over ~20 hours. This time dependence suggests a diffusional limitation that cannot be attributed to gas-phase diffusion. Therefore, the purification rate must be limited by the diffusion rate of silicon from the bulk to the surface of the alloy. Although the transport rate values plotted were determined by the time-average method, they agree with the real-time measures since the total run time was held constant.

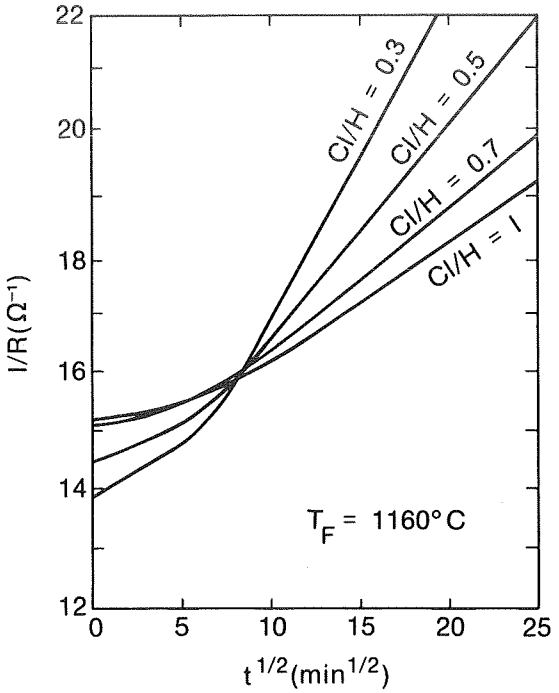

Figure 3. Real-time plot of the filament conductance as a function of $t^{1/2}$ for four different Cl/H ratios.

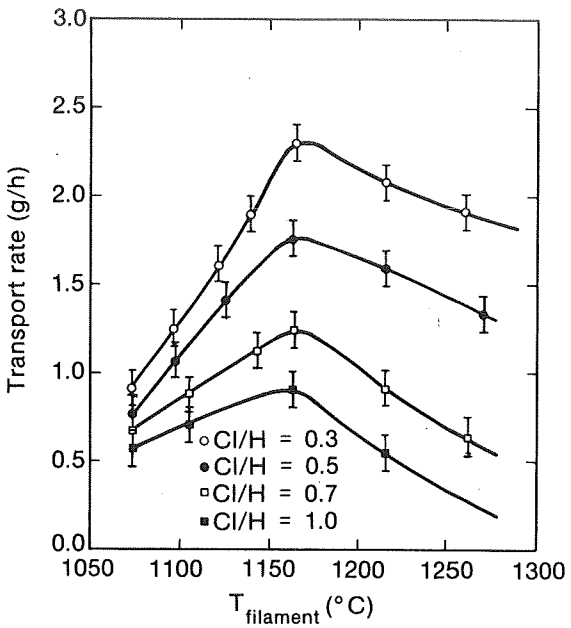

Figure 4. Average-time transport rate as a function of the filament temperature for Cl/H = 0.3 to 1.0.

For any given Cl/H ratio, we observe that the transport rate exhibits an asymmetric maximum around 1160°C (see Figure 4). Since the alloy temperature scales with the filament temperature, the increase in rate with increasing filament temperature below the maximum is attributed to the increased diffusivity of Si within the alloy. However, the gas-phase solubility of Si near the alloy decreases with increasing temperature (7). This tends to decrease the rate since the surface concentration of Si in the alloy presumably is an inverse function of the local gas-phase solubility. Furthermore, the gas-phase solubility passes through a minimum with increasing temperature. Thus, the difference in gas-phase solubility between the alloy and the filament, which drives the gas-phase transport, passes through a maximum and then decreases to zero with increasing temperature for a given temperature difference between alloy and filament. This is observed experimentally at very high temperatures where no deposition occurs. Thus, at low temperatures the rate is controlled by Si diffusion in the alloy and is fairly insensitive to Cl/H. At higher temperatures the rate passes through a maximum due to the competing effects of larger diffusivity within the alloy but lower driving forces for both diffusion through the alloy depletion layer and for gas-phase transport. At very high temperatures, gas-phase transport controls the rate. In fact, the driving force for gas-phase diffusion, which is sensitive to Cl/H, inverts and no deposition occurs.

The optimum Cl/H ratio appears to be near 0.3. At lower values the deposits can become dendritic, and of course as Cl/H approaches zero so does the rate. At higher values of Cl/H, the relative concentration of $SiCl_2$ increases. Since the formation reaction of HCl with Si to form $SiCl_2$ is endothermic, this reaction

tends to transport Si from the filament to the alloy. Thus, at higher Cl/H we expect the transport rate to diminish. A growth rate as high as 2.3 g/h has been achieved for Cl/H = 0.3 and deposition temperatures of 1160°C.

SUMMARY

The vapor-transport filtration (VTF) process permits the production of 99.9999% pure silicon from metallurgical-grade silicon, which is suitable for solar cells. The purification efficiency is attributed to four mechanisms: gettering of impurities during casting of the alloy, the chemical selectivity of the HCl vapor-transport process, the unusual filtration properties of Cu_3Si, and the condensation of impurities in the form of chlorides on the cold walls and baseplate of the reactor. Optimum growth rates occur at deposition temperatures around 1160°C and a Cl/H ratio of 0.3.

The VTF technique is a closed-cycle process that is adapatable to small- or large-scale operations requiring only a small volume of HCl and H_2 and Si:Cu_3Si composite alloys as inputs. There are no large volumes of waste gas to recycle or dispose of, and the spent copper alloy can easily be recycled by means of common metallurgical processes.

ACKNOWLEDGMENTS

The authors would like to thank T. F. Ciszek for growing the single crystals, T. Schuyler for the cell processing, and C. Osterwald for the cell measurements. This work was supported by the U.S. Department of Energy under contract no. DE-AC02-83CH10093 and by the Instituto de Electronica de Comunicaciones (C.S.I.C), Madrid, Spain.

References

1. Olson, J.M., and K.L. Carleton, "A Semipermeable Anode for Silicon Electrorefining," J. Electrochem. Soc., Vol. 128, No. 12, Dec. 1981, pp. 2698-2699.
2. Olson, J.M., "Silicon Electrorefining and the Transport Properties of Cu_3Si," Proc. of the Fourth Symposium on Materials and New Processing Technologies for Photovoltaics, Vol. 83-11, edited by J.A. Amick, V.K. Kapur, and J. Dietl, Pennington, NJ: Electrochem. Soc., 1983, pp. 119-131.
3. Olson, J.M., and R.C. Powell, "A Vapor Transport Filtration Technique for Purifying Silicon," 17th IEEE Photovoltaics Specialists Conf., New York, NY, IEEE, 1984, pp. 1143-1145.
4. Powell, R.C., 1984, Silicon Purification Using Chemical Vapor Transport From a Copper-Silicon Alloy Source, M.S. Thesis, Golden, CO: Colorado School of Mines.
5. Schäfer, Harald, Chemical Transport Reactions, New York, NY: Academic Press, 1964, pp. 30-114.
6. van Arkel, A.E., and J.H. de Boer, "Darstellung von reinem Titanium-, Zirkonium-, Hafnium- und Thoriummetall," Z. anorg. u. allgen. Chem., Vol. 148, 1925, pp. 345-350.

7. Bloem, J., Y.S. Oei, H.H.C. de Moor, J.H.L. Hanssen, and L.J. Giling, "Near Equilibrium Growth of Silicon by CVD. I. The Si-Cl-H System," J. Cryst. Growth, Vol. 57, Nos. 1-3, Dec. 1983, pp. 399-405.
9. Hunt, L.P., and E. Sirtl, "A Thorough Thermodynamic Evaluation of the Silicon-Hydrogen-Chlorine System," J. Electrochem. Soc., Vol. 119, No. 12, Dec. 1972, pp. 1741-1745.
10. Lever, R.F., "The Equilibrium Behavior of the Silicon-Hydrogen-Chlorine System," IBM J. Res. Develop., Vol. 8, Sept. 1964, pp. 460-465.
11. Rolsten, R.F., Iodide Metals and Metal Iodides, New York: John Wiley & Sons, 1961, pp. 273-292.
12. Kibbler, A., R.C. Powell, and J. M. Olson, to be published.

C-5